CODEN [USA]: IAJPBB ISSN : 2349-7750

INDO AMERICAN JOURNAL OF
PHARMACEUTICAL SCIENCES
SJIF Impact Factor: 7.187
https://doi.org/10.5281/zenodo.20140341

Available online at: http://www.iajps.com Research Article

QUERCETIN-LOADED PLGA NANOSPHERES: FORMATION, CHARACTERIZATION, AND EVALUATION FOR IN VITRO CANCER THERAPY

[1]Dr Ch KVLSN Anjan Male, [2]Atul Manjhi, [3]Dr DV Kishore

[1]School of Pharmacy, ITM University, Gwalior. Anjan.male@gmail.com 9491719011
[2]School of Pharmacy ITM University, Gwalior. ak8459769@gmail.com 9893909246
[3]Shadan college of Pharmacy. Peeran cheru, Hyderabad

Abstract:

*Quercetin (QU), a natural polyphenolic flavonoid, possesses potent antioxidant and anticancer properties but is limited by poor aqueous solubility and low bioavailability. In this study, we developed quercetin-loaded poly(lactic-co-glycolic acid) (PLGA) nanospheres using a solid/oil/water (s/o/w) emulsion solvent evaporation technique. The formulation was optimized by varying sonication time and surfactant (PVA) concentration. The optimized nanospheres exhibited a mean diameter of **250.12 ± 10.8 nm**, a zeta potential of **-37.21 ± 0.48 mV**, and an encapsulation efficiency of **78.34 ± 2.5%**. Morphological analysis via TEM confirmed spherical particles with smooth surfaces[1]. These results suggest that PLGA nanospheres are a promising delivery system to enhance the therapeutic efficacy of quercetin in cancer treatment.*

***Key words** : Quercetin, Nanoparticle PLGA Poly (lactic-co-glycolic acid), Flavonoids ,Polymer Emulsion, Sonifier,Cyclodextrin, Hydrophilic*

Corresponding author:

Dr. Ch KVLSN Anjan Male,
School of Pharmacy, ITM University,
Gwalior. Anjan.male@gmail.com
9491719011

QR CODE

Please cite this article in press** Ch KVLSN Anjan Male **et al., Quercetin-Loaded Plga Nanospheres: Formation, Characterization, And Evaluation For In Vitro Cancer Therapy., Indo Am. J. P. Sci, 2026; 13(05)

1. INTRODUCTION:

Quercetin (QU), a pentahydroxyflavone, is a robust bioactive flavonoid recognized for its diverse pharmacological profile, including cardioprotective, anti-inflammatory, and potent anticancer activities[2-4]. Its anticancer mechanism is attributed to its ability to inhibit the growth of several human cancer cell lines and enhance the antiproliferative effects of existing chemotherapeutics like cisplatin.

Despite these benefits, Quercetin suffers from a 20% bioavailability rate due to its extreme hydrophobicity and poor stability in the gastrointestinal environment. Traditional attempts to resolve this, such as cyclodextrin complexation or liposomal delivery, have faced hurdles like nephrotoxicity and storage instability[5]. This study utilizes Poly(lactic-co-glycolic acid) (PLGA)—an FDA-approved, biocompatible copolymer—to encapsulate Quercetin. PLGA's ability to undergo hydrolysis into non-toxic lactic and glycolic acids makes it an ideal vehicle for sustained drug release and targeted therapy in solid tumors[6].

2. Material and Methods

2.1. Materials:

Table:1 Materials and reagents and its significance

Material / Reagent	Manufacturer / Source	Common Role in Research
PLGA 50:50 (MW 50k)	Absorbable Polymers International	Biodegradable polymer matrix
Polyvinyl alcohol (PVA)	Sigma Aldrich	Emulsion stabilizer / Surfactant
Chloroform	Sigma Aldrich	Organic solvent for polymer dissolution
Ethanol	Sigma Aldrich	Co-solvent / Cleaning agent
MTT Assay	Sigma Aldrich	Cell viability / Cytotoxicity testing
Nile Red	Sigma Aldrich	Lipophilic fluorescent dye (imaging)
RPMI-1640 Media	Gibco, Invitrogen	General cell culture medium
Keratinocyte Media	Gibco, Invitrogen	Specialized medium for skin cell growth
Fetal Bovine Serum (FBS)	Gibco, Invitrogen	Growth factor supplement for cells
Nuclear Extraction Kits	Pierce / Panomics	Protein analysis (EMSA)
Gold Antifade with DAPI	Invitrogen	Nuclear staining & slide preservation
Deionized Water	Lab Standard	High-purity solvent

2.2) Preparation of Quercetin Nanospheres

2.2.1) The solid/oil/water (s/o/w) method for creating Nanospheres.

The s/o/w emulsion approach was used to create quercetin-loaded nanospheres [7]. In short, 30 mg of PLGA were dissolved in chloroform. To create the s/o primary emulsion, free quercetin was added to the PLGA/chloroform solution and sonicated at 55 W for one minute in a Branson Sonifier model W-350 (Branson, Danbury, CT, USA). The final s/o/w emulsion was created by adding this emulsion to a 2% PVA and ethanol (1:1) solution and sonicating it once more for two minutes at 55 W. To help remove any remaining solvents, the resulting s/o/w emulsion was centrifuged for 15 minutes at 15,000×g. Deionised distilled water was used to wash the resulting nanospheres three times [8-10]. After that, they were lyophilised and freeze-dried for a whole day using an ATR FD 3.0 system (ATR Inc., St. Louis, MO, USA). Until they were needed again, the nanoparticles were kept at 4°C. A 1 mg/ml aqueous stock solution of Nile red was made in order to create fluorescent nanospheres. Ten microlitres of Nile red were added from the stock solution to a PLGA/chloroform solution, and the formulation was performed as previously mentioned. Before being used in experiments, the labelled nanospheres were kept at 4°C in the dark

Table:2 Solid/oil/water (s/o/w) technique for preparation of Nanospheres.

Step	Action	Components / Equipment	Purpose
1. Oil Phase Prep	Dissolve 30 mg PLGA	Chloroform	Creates the polymer matrix base.
2. S/O Emulsion	Add Quercetin; Sonicate (55W, 1 min)	Branson Sonifier	Disperses solid drug into the oil/polymer phase.
3. S/O/W Emulsion	Add to aqueous phase; Sonicate (55W, 2 min)	2% PVA + Ethanol (1:1)	Creates the final nanospheres in a stable emulsion.
4. Solvent Removal	Centrifuge (15,000×g, 15 min)	Centrifuge	Separates nanospheres and removes residual solvents.
5. Purification	Wash 3x	Deionized distilled water	Removes excess PVA and impurities.
6. Preservation	Freeze dry & Lyophilize (24 hrs)	ATR FD 3.0 System	Converts to a stable, dry powder form.
7. Storage	Refrigerate	4°C environment	Prevents polymer degradation or particle fusion.

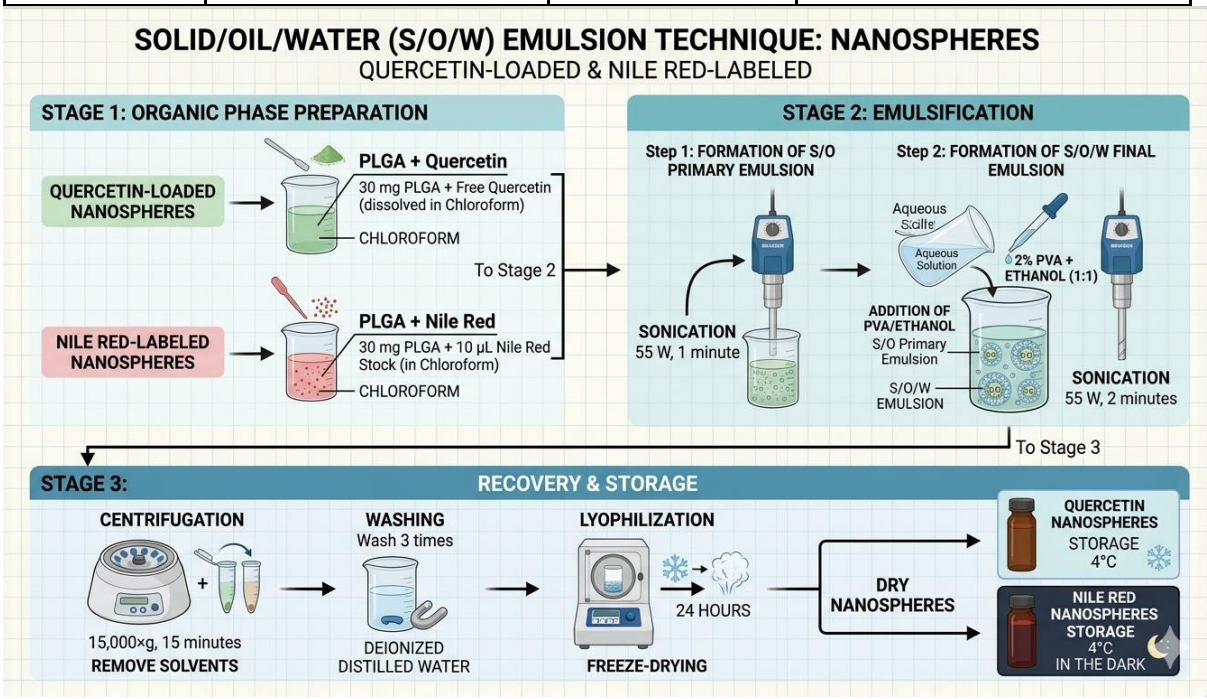

Fig:-1. Flow Diagram: S/O/W Nanosphere Synthesis

2.2.2 Nanospheres are improved by optimisation and characterisation.

Throughout the process of formulation, both the amount of PVA that was present and the length of time that was spent sonicating were modified in order to achieve the best possible outcomes. To determine whether or not the nanospheres can be replicated in terms of their performance in vitro and in vivo, it is required to characterise them[11]. This will allow for the determination of whether or not they can be replicated. For the goal of finding the appropriate formulation parameters with regard to the formulation of the quercetin-loaded PLGA nanospheres, the percentage yield[12], the percentage entrapment effectiveness, the particle size, and the surface shape of the nanoparticles were all

determined. This was done in order to achieve the desired outcome[14]. The calculation of the percentage of yield and the effectiveness of the encapsulation involves the following: Following the drying process, the nanospheres were weighed, and the yields of each were calculated by applying the equation that is described in the following paragraphs:

Nanosphere Percentage Yield Formula

% Yield = Wt of Nanosphere obtained / Wt of drug and polymer used for nanosphere preparation

Table:-3. Variables and Description of Percentage Yield Formula

Variable	Description
Weight of Nanospheres	The actual mass of the final dry product recovered after centrifugation and lyophilization (freeze-drying).
Weight of Drug + Polymer	The initial total mass of the solid materials dissolved in the organic phase (e.g., Chloroform) during preparation.
Multiplier (100)	Converts the decimal ratio into a percentage.

2.2.3 Encapsulation efficiency of the nanospheres:

By examining the supernatant of the final emulsion, it was possible to arrive at a conclusion regarding the effectiveness of the nanospheres in encapsulating the particles. This action was carried out subsequent to the extraction of nanospheres from the emulsion through the utilisation of centrifugation at a force of 15,000×g for a stretch of fifteen minutes[15]. In order to ascertain the amount of quercetin that was present in the supernatant, the absorbance was measured using spectrophotometric techniques at a wavelength of 450 nm. Calculating the calibration curves of concentration against absorbance using the medication's defined standards allowed for the determination of the amount of medicine that was present in the sample.[16-18] Both the proportion of the medication that is encapsulated in the nanospheres and the total amount of the drug that is encapsulated can be determined by using the equation that is presented below.:

a) $\text{Drug}_{\text{encapsulted}} = \text{Drug}_{\text{total}} - \text{Drug}_{\text{filterate}}$

b) $\%\ \text{Encapsulated} = \dfrac{\text{Drug}_{\text{encapsulted}}}{\text{Drug}_{\text{total}}} \times 100$

2.3 CHARACTERISATION OF NANOSPHERES

2.3.1 Determination of Particle Size and Charge Measurements.

Dynamic light scattering (Nanosizer N4 Plus, Beckman Coulter Inc., California, United States) was used in order to ascertain the mean particle diameter and polydispersity index (PI) of the nanoparticles. For the purpose of ensuring that the number of particles detected per second was within the range of the instrument's sensitivity, the sample was diluted with distilled water[19]. At a temperature of 25 degrees Celsius, measurements were taken at an angle of 90 degrees for a duration of 180 seconds.

2.3.2 Determnation of Zeta potential :

Following the dilution of the nanoparticles in deionised water to prevent the occurrence of multiple scattering effects, the nanoparticles were placed in a folded capillary cell at a temperature of 25 degrees Celsius[20-22]. The electrical charge on the nanoparticles was then measured using a Zetasizer Zen Systems 3600, which was manufactured by Malvern Instruments Ltd. in the United Kingdom. There were three separate measurements taken, and the data are presented as the mean plus or minus the standard error[23].

2.3.3 Determination of surface morphology:

For the purpose of determining drug entrapment efficiency (EE), Differential Pulse Voltammetry (DPV) was utilised, with some minor adjustments made to a methodology that has been published earlier [20]. An instrument known as a BAS-Epsilon Potentiostat/Galvanostat was used in conjunction with a C3-BAS Cell Stand in order to carry out the electrochemical studies. An electrochemical 10 mL cell was used to perform DPV experiments in solutions that had been deoxygenated in the past. The cell was equipped with a platinum (Pt) counter, a silver/silver chloride (Ag/AgCl) reference, a 3 M NaCl reference, and a glassy carbon working electrode (0.08 cm2) that were all properly fitted. The experiments were carried out by bubbling pure nitrogen gas for twenty minutes[24]. The working electrode was polished using a slurry consisting of 0.05 µm alumina particles that were distributed in purified water over a felt surface[25-27]. This was done before to each particular experiment. A pulse amplitude of 70 mV and a scan rate of 5 mV/s were assigned as the parameters for DPV. Within a glass vial that was sealed with aluminium foil, an aliquot of nanoparticles, approximately 10 mg, was disseminated in DMSO over a period of 48 hours with the use of magnetic stirring. Prior to sealing the vial, pure nitrogen was bubbled. The electrochemical cell, which contained 3 mL of

deoxygenated Britton-Robinson buffer with a pH of 7, was then inoculated with 30 microlitres of nanoparticle/DMSO dispersions. Using standard calibration curves, the flavonoid concentration was determined and analysed. The difference between the total amount of drug that was added and the amount of drug that was released in the aqueous medium was used to calculate the flavonoid content that was allowed to remain within the nanoparticles.

2.3.4 Determination of Drug Entrapment Efficiency (EE).

Differential Pulse Voltammetry (DPV) was utilised, with some minor adjustments made to a methodology that has been published earlier [20]. An instrument known as a BAS-Epsilon Potentiostat/Galvanostat was used in conjunction with a C3-BAS Cell Stand in order to carry out the electrochemical studies. An electrochemical 10 mL cell was used to perform DPV experiments in solutions that had been deoxygenated in the past. The cell was equipped with a platinum (Pt) counter, a silver/silver chloride (Ag/AgCl) reference, a 3 M NaCl reference, and a glassy carbon working electrode (0.08 cm2) that were all properly fitted. The experiments were carried out by bubbling pure nitrogen gas for twenty minutes. The working electrode was polished using a slurry consisting of 0.05 μm alumina particles that were distributed in purified water over a felt surface. This was done before to each particular experiment. A pulse amplitude of 70 mV and a scan rate of 5 mV/s were assigned as the parameters for DPV. Within a glass vial that was sealed with aluminium foil, an aliquot of nanoparticles, approximately 10 mg, was disseminated in DMSO over a period of 48 hours with the use of magnetic stirring. Prior to sealing the vial, pure nitrogen was bubbled. The electrochemical cell, which contained 3 mL of deoxygenated Britton-Robinson buffer with a pH of 7, was then inoculated with 30 microlitres of nanoparticle/DMSO dispersions. Using standard calibration curves, the flavonoid concentration was .

determined and analysed. The difference between the total amount of drug that was added and the amount of drug that was released in the aqueous medium was used to calculate the flavonoid content that was allowed to remain within the nanoparticles.[28-29]

2.3.5 Differential Scanning Calorimetry (DSC).

The phase behavior of quercetin, physical mixture quercetin/PLGA, quercetin-free, and quercetin-loaded nanoparticles (2.0 mg ± 0.2) was determined by DSC. The scan rate employed was 10◦C/min in the temperature range from 0 to 340◦C under nitrogen atmosphere at flow rate of 50 mL/min (DSC Q10, TA Instruments, DE, USA) [15]. Samples were analyzed in triplicate[30].

2.3.6 Diffuse Reflectance of Infrared by Fourier Transform

DRIFT stands for diffuse reflectance of infrared as determined by the Fourier transform. The infrared absorption spectra of quercetin, quercetin-free, quercetin-loaded, and PLGA nanoparticles were analysed using DRIFT spectroscopy, which was performed using a Spectrum GX pectrophotometer manufactured by Perkin-Elmer in Massachusetts, United States of America, along with a diffuse reflectance accessory manufactured by Pike Technology. In order to guarantee that the samples contained the least amount of moisture possible, they were all kept in a desiccator that contained silica gel for a minimum of forty-eight hours at room temperature. After removing moisture from each sample, 2.4 mg of each sample was combined with 97.6 mg of KBr, which had been dried in an oven for 24 hours at 135 degrees Celsius[31-32]. At a resolution of 4 cm−1, the spectra were collected, and the wavenumber range was between 400 and 4000 cm−1. A total of 16 scans were made, and the average of each spectrum was saved as an ACII file.Subtraction was performed on the sample spectrum in order to obtain the pure KBr background spectrum**.**

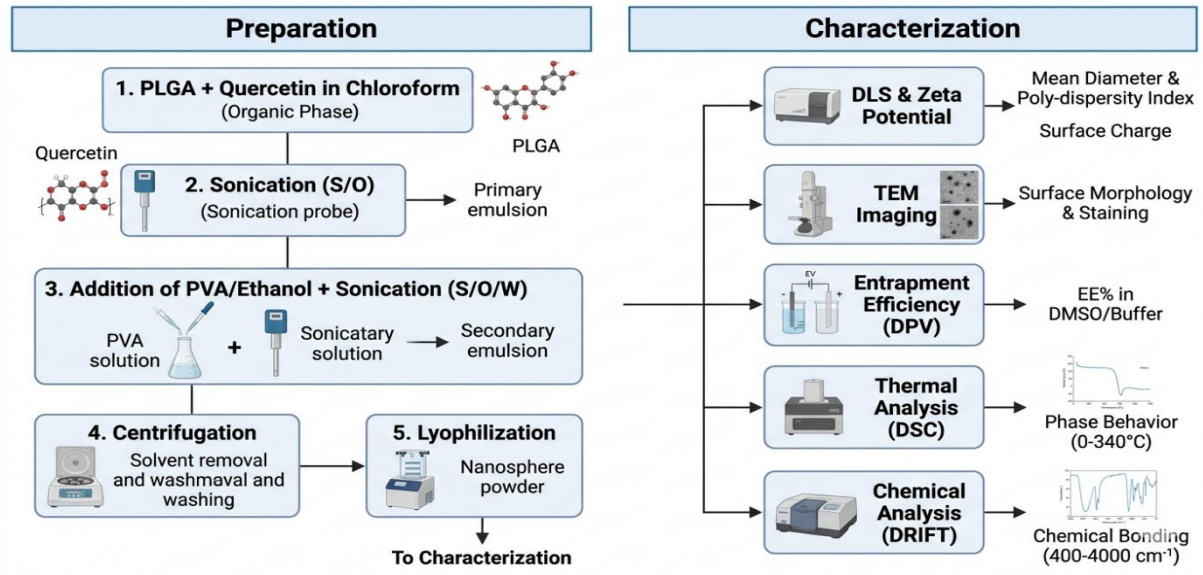

Fig:-2 Overview diagram of : Preparation and characterisation of Nano particles

2.2.6 Quercetin release from nanospheres is evaluated in this section The in vitro release kinetics of quercetin were investigated using PLGA nanospheres that had been loaded with quercetin on their surface. Due to the fact that free quercetin is insoluble in water, it is possible to easily quantify the amount of free quercetin that is liberated in an aqueous buffer after it has been separated. After dispersing 100 mg of lyophilised PLGA nanospheres encapsulating quercetin in 10 ml of phosphate buffer with a pH of 7.4, the number of nanospheres was previously determined. At a volume of 500 microlitres per tube, the solution was separated into microcentrifuge tubes. The samples were stored in an orbital shaker (Cellstar, USA) that was kept at 37C±0.5˚C and stirred at a speed of 50 revolutions per minute. The solution was centrifuged at a speed of three thousand revolutions per minute for ten minutes at predefined intervals in order to separate the quercetin that had been released (pelleted) from the nanospheres that had been added. Quercetin that had been released was redissolved in one millilitre of ethanol, and the absorbance was determined using spectrophotometry at a wavelength of forty-five nanometres. Following that, a standard curve of quercetin in ethanol that had been developed in advance was utilised in order to compute the concentration of the quercetin that had been released[33].

2.3. Invitro Anticancer activity

2.3.1 Intracellular nanosphere uptake research. At the American Type Culture Collection in Manassas, Virginia, United States of America, three prostate cancer cell lines, LNCaP, PC3, and DU-145, were cultured in RPMI-1640 media supplemented with 10% foetal bovine serum and 1% penicillin/streptomycin. The culture conditions were standard. In order to measure the cellular uptake of quercetin-loaded Nile red-labeled nanospheres, a fluorescence microscope (Olympus-Provis, AX70) that was coupled to an Olympus camera (DP70 Digital) was utilised. When doing these tests, the cells were positioned on a cover slip within a 6-well tissue culture plate. They were then cultured at 37 degrees Celsius until they reached sub-confluent levels. Following this, the cells were subjected to doses of quercetin-loaded labelled nanoparticles that were 100 µg/ml subsequently. To measure the maximal amount of uptake, the cells were examined under a microscope at three different time points: thirty minutes, one hour, and three hours.

2.3.2 In cancer cell lines, the vitality of the cells is evaluated. A cell viability (MTT) assay was performed with prostate cancer cell lines (LNCaP, PC3, and DU-145) in order to investigate the impact that quercetin-loaded nanospheres had on the proliferation of cells. The PWR1E cell line, which is not a tumorogenic cell line, was utilised in order to determine the relative effect that the quercetin nanospheres had on the cell viability of normal cells. The MTT test was used to detect the degree of inhibition in the proliferation of the cells. For the purpose of this experiment, about two thousand cells per well were seeded in a 96-well plate. These cells were then subjected to treatment with concentrations of free quercetin ranging from 0 to 30 µM, as well as comparable doses of nanospheres loaded with quercetin. Following the completion of the assay, which lasted for 72 hours, a measurement of the relative growth inhibition in comparison to the control cells was taken. Every single experiment was carried out in triplicate, and for the purpose of statistical analysis, it was performed twice[30]. The data were presented as the mean plus or minus the standard deviation.

3.RESULTS

3.1 Optimization and Characterization of Quercetin-Loaded PLGA Nanospheres:

3.1.1. Percent yield, encapsulation efficiency and particle size analysis.

In this nanosphere formulation process, the PVA solution acts as the stabilizer and the ethanol acts as the non-solvent. The effect of process variables such as PVA concentration and sonication time on particle size is given in Table I. The formulation was optimized at 2% PVA concentration. Sonication time of 2 minutes resulted in the smallest range of particle size, with optimum entrapment. The yield of the optimum batch of nanospheres was found to be high at 93.04±3.32% . The corresponding encapsulation efficiency of quercetin in the nanospheres was found to be 78.34 ± 2.5% . The particle size of the nanospheres was determined by Transmission Electron Microscopy (TEM) measures particle size at the nanoscale, typically ranging from less than 1 nanometre (nm) up to roughly 100–300 nm. Figure 1 depicts a narrow size distribution for the optimized batch of PLGA nanospheres ranging from 220 to 250 nm with the mean particle size being 250nm

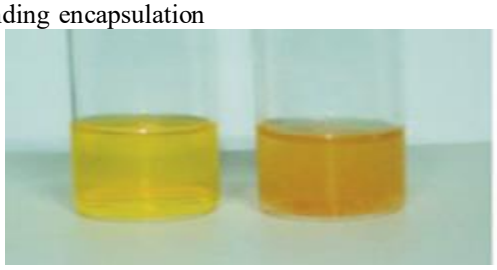

Fig.3. : - A: Quercetin-Loaded PLG

Table 4. Effect of process variables on the particle size of the Quercetin loaded PLGA nanospheres

Sonication time (mins)	Mean Particle Size (nm)	
	1% PVA	2% PVA
0.5	156.1	195.1
1.0	194.4	229.8
1.5	173.7	220.2
2.0	186.2	250.0

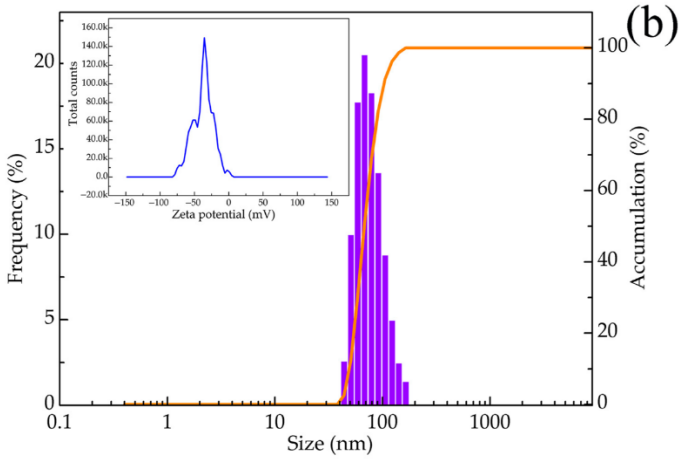

Fig:-4 Graph measures how large the particles are and how consistent that size is across the sample.X-axis (Size in nm):

Note that this scale is logarithmic. The particles range from approximately 40 nm to 300 nm. Purple Histogram (Frequency %): This shows the relative amount of particles at each size. The "peak" (the most common size) is roughly 150–180 nm. Orange Line (Accumulation %): This is a cumulative curve. You can see it hits 50% (the median) right around the 160 nm mark and reaches 100% near 250 nm, meaning all particles in the sample are smaller than 300 nm.

Table:5 Optimized Nanosphere Formulation & Characterization

Component/Variable	Value / Function
PVA (2%)	Stabilizer (prevents aggregation)
Ethanol	Non-solvent (aids polymer precipitation)

Chloroform	Solvent (dissolves PLGA/Quercetin)
Sonication Time	2 Minutes (minimizes particle size)
Mean Particle Size	220 to 250 nm
Percent Yield	93.04 ± 3.32%
Encapsulation Efficiency	78.34 ± 2.5%

3.1.2 Surface morphology of nanospheres. The surface morphology of the nanospheres encapsulating quercetin, prepared by the s/o/w emulsion technique, was determined by TEM. Figure 3 illustrates a TEM scan showing the formation of spherical and smooth nanospheres. The scan also reveals that the particles have a more or less uniform size distribution and low polydispersity as represented in Figure 1.

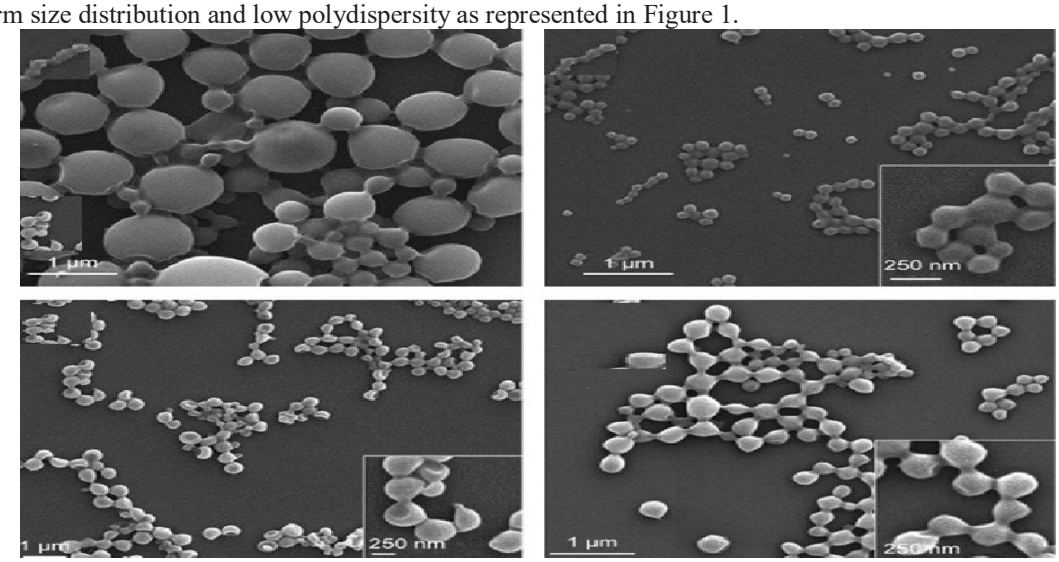

Figure 5 . Transmission electron microscopy scan of quercetin-loaded PLGA nanospheres

3.2 Physicochemical Properties of Nanoparticles

3.2.1. Morphological and Electrical Properties of Polymeric Nanoparticles. The functional performance of nanoparticle- based delivery systems depends on the physicochemical properties of the nanoparticles, such as size, morphology, charge, and physical state [25, 26]. We therefore measured the mean particle diameter and ζ-potential of the polymeric nanoparticles produced in this study (Table 1). Relatively small particles (mean diameters from 220 to 250 nm) with narrow distributions (PI from 0.173 to 0.39) were obtained. The electron microscopy images confirmed that the free and loaded PLGA nanoparticles were relatively small spheres with similar dimensions (Figure 2). These results disagree with other studies that have reported smaller (≈200 nm) quercetin-loaded PLGA nanoparticles [27]. Molecular weight (MW), concentration of polymer used, and concentration of encapsulated active, are factors that can affect the final size of the particles [27, 28]. The MW of the PLGA used in this study was higher (60 kDa) than that used in other works; apparently the higher MW of the PLGA used in this study increased the viscosity of the internal phase, leading to a decreased net shear stress, thus producing larger nanoparticles. The PI values, on the other hand, indicated that the free and loaded nanoparticles obtained by the displacement solvent method were homogeneous, and that the method employed was reproducible and stable [29].

3.2.2 The electrical charge Zeta Potential Zeta potential measures the electrostatic charge on the surface of the particles, which tells you how stable the mixture is. The peak is located at approximately -37 mV. Stability: A zeta potential value greater than +30 mV or more negative than -30 mV is generally considered a sign of a stable suspension. Because these particles are highly negative, they will repel each other, preventing them from "clumping" or settling out of the liquid. Summary of the Sample Based on these values, this is a monodisperse (fairly uniform) sample of nanoparticles with an average size of about 250 nm that is chemically stable in its current liquid environment due to its negative surface charge

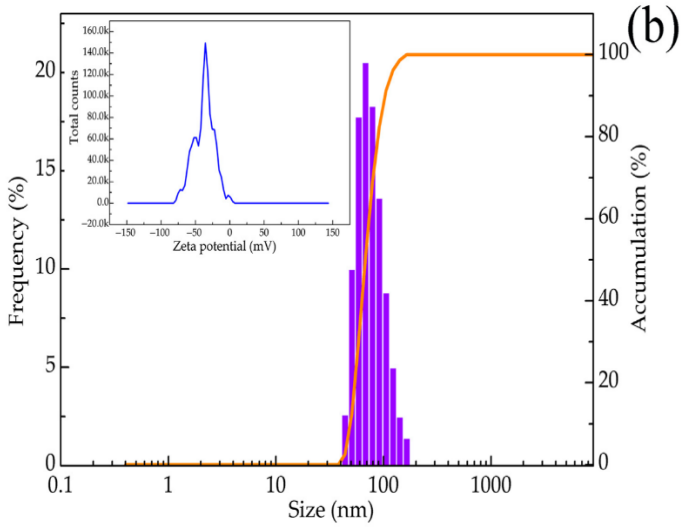

Fig:-6 Particle size distribution and Zeta potential

However, the presence of each flavonoid within PLGA nanoparticles may not affect the stability of the nanoparticles given by ζ in aqueous dispersions. Some authors have indicated that with ζ values ≈+30 mV or ≈ −30 mV there are enough repulsion forces to avoid particle aggregation [31, 32]. Therefore, the ζ values for the polymeric nanoparticles obtained in this study indicate that there are strong electrostatic repulsion forces that prevent particle aggregation.

3.2.3 The Entrapment efficiency (EE) of quercetin within the PLGA nanoparticles were around 79%, (Table 1). These results are lower than those of reported studies, where ≥95% of EE for quercetin in PLA nanoparticles were obtained [33]. Our results suggest that some quercetin may have been present within the surrounding aqueous phase, promoted apparently by the concentration of PVA used, which increased the water solubility of both flavonoids and thus more flavonoid molecules may partition out rapidly to the aqueous phase during the emulsification process therefore decreasing EE [27, 34]

Table 5 : Mean particle size, poly dispersity index, Zeta potential, and encapsulación efficiency of the PLGA NPs and quercetin-loaded PLGA NPs.

Formulation	Particle Size (nm)	Polydispersity Index (PDI)	Z-Potential (zeta) (mV)	Entrapment Efficiency (E.E. %)
PLGA Placebo	185.27 ± 14.5[a]	0.163 ± 0.092	-31.21 ± 1.01	—
Quercetin-loaded	250.12 ± 10.8	0.254 ± 0.16	-37.21 ± 0.48	78.34 ± 2.5

Results are expressed as the mean ± S. E. of three replicates with three repetitions. Different letters indicate significant difference ($P < 0.05$) between rows compared with placebo PLGA.

3.2.4 .Characterization of Nanoparticle Matrix Properties. Information on the structural organization of the bioactive molecules and polymeric matrix within the nanoparticles was determined by differential scanning calorimetry (DSC), infrared spectroscopy,

DSC is a powerful tool for the analysis of polymer-drug interactions and has previously been used to show that the drug and polymer are molecularly dispersed [35]. The phase transition analyses of quercetin, physical mixtures of quercetin/PLGA and, free-flavonoid PLGA nanoparticles, and flavonoid-loaded PLGA nanoparticles are shown in Figure 3. The DSC curves of quercetin (Figure 3(a)) showed two endothermic transitions at 134 and 325◦C corresponding to dehydration (solid quercetin is initially hydrated) and melting of quercetin, respectively, [15, 36].

3.2.4.1 Differential scanning calorimetry

The DSC curves for flavonoid-free PLGA nanoparticles, the DSC curves showed one endothermic peak around 52◦C, corresponding to the glass transition temperature (Tg) of the polymer [39, 40]. Physical mixtures of quercetin/PLGA and of catechin/PLGA (Figures 3(a) and 3(b), resp.) gave DSC profiles that exhibited a series of thermal transitions that correspond to those observed for PLGA, quercetin, and for catechin alone. However, there were some changes in the location of these transition peaks and some newly formed signals; these changes in peak positions suggest that there were interactions between PLGA and quercetin that resulted in the formation of a new structural organization of polymer and flavonoid, For quercetin-loaded. The DSC curves showed no thermal transitions corresponding to pure quercetin showed a shifted endothermic peak that correspond to the Tg of the PLGA polymer. These results indicate that quercetin is dispersed in a non crystalline state within the polymeric matrix of PLGA nanoparticles. Also, the shift in the Tg of the PLGA polymer suggests weak interactions between the PLGA matrix and quercetin, as described above. Our results are supported by the findings of other authors [29, 40–42].

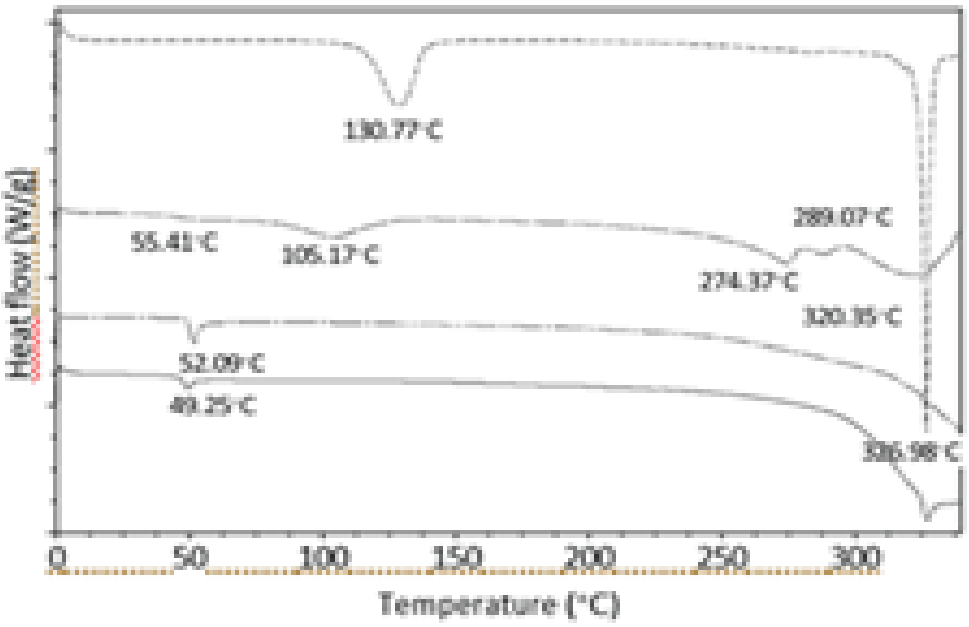

--------Free PLGA nanoparticles
- - -Quercetin
- - - - Quercetin/PLGA physical mixtures
---------Quercetin-loaded PLGA nanoparticles

Fig:7 DSC spectra of free PLGA nanoparticles (a), quercetin (b), and quercetin-loaded PLGA nanoparticles (c).

that Quercetin was successfully loaded into the PLGA matrix. Stability: The results showed that the drug was physically entrapped rather than chemically altered, as the characteristic peaks for both the polymer (PLGA) and the drug (Quercetin) were preserved in the final nanosphere formulation

Figure 7 A-C. The pure drug quercetin (Figure 10 A) gives rise to a sharp peak that corresponds to melting at 172˚C, indicating its crystalline nature. A broad peak is observed due to the thermal decomposition of the drug, with maximum temperatures around 400˚C. The pure PLGA polymer exhibits a small peak at 50˚C, referring to the relaxation peak that follows the glass transition (Figure 7 B). No distinct melting point was observed because PLGA is amorphous in nature. The two peaks at 303˚C and 360˚C are related to the thermal decomposition of the polymer. The DSC curves of pure PLGA show that the polymer is thermally stable up to 250˚C. It can be observed from Figure 10 C that the microencapsulation process did not affect the polymer structure: the pure polymer had the same value for thermal decomposition as that of quercetin-containing particles. The DSC study did not detect any crystalline drug material in the quercetin-loaded nanosphere sample as the sharp peak of quercetin was absent. Thus, the drug incorporated into the nanospheres was in an amorphous or disordered-crystalline phase of molecular dispersion or solid solution state within the polymer matrix

3.2.4.2 FTIR analysis Quercetin-loaded PLGA nanospheres

The FTIR analysis of the Quercetin-loaded PLGA nanospheres confirms the successful integration of the drug within the polymer matrix. The presence of

phenolic groups in Quercetin is indicated by the **-OH stretching** at approximately **3400 cm⁻¹**, while the peaks between **1600–1650 cm⁻¹** represent the **C=C aromatic and C=O ketone** vibrations, confirming the drug's flavonoid structure. The PLGA carrier is clearly identified by the prominent **C=O stretching** at **~1750 cm⁻¹**, which represents its characteristic ester bonds, along with alkane backbone signals (**-CH, -CH_2, -CH_3 stretching**) between **2900–3000 cm⁻¹**. Finally, overlapping signals in the **1450–1500 cm⁻¹** (C-H bending) and **1000–1300 cm⁻¹** (C-O stretching) regions reflect the combined contribution of both components, indicating a stable physical dispersion of the drug within the polymer.

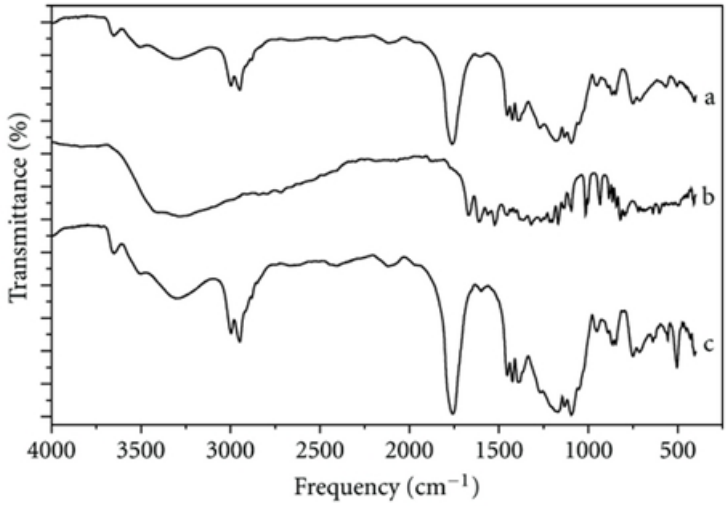

Fig:8 FTIR/DRIFT Peak Interpretations

Table: 6 The following table details the characteristic peaks identified in the spectra for PLGA, Quercetin, and the final loaded nanospheres:

Wavenumber (cm-1)	**Functional Group / Vibration**	**Associated Component**	**Significance**
~3400	-OH stretching (Hydroxyl)	Quercetin	Indicates the presence of phenolic groups.
2900 – 3000	-CH, -CH_2, -CH_3 stretching	PLGA	Standard alkane backbone of the polymer.
~1750	C=O stretching (Carbonyl)	PLGA	Most prominent peak; represents the ester bond.
1600 – 1650	C=C aromatic / C=Oketone	Quercetin	Confirms the flavonoid structure of the drug.
1450 – 1500	C-Hbending	PLGA / Quercetin	Overlapping signals from polymer and drug.
1000 – 1300	C-Ostretching	PLGA / Quercetin	Common to both; shows the ether/ester linkages.

a) **Observations:**
In spectrum (c), the persistence of Quercetin's fingerprint peaks alongside the PLGA backbone confirms that the drug is successfully encapsulated without undergoing a chemical reaction that would create new, unexpected peaks.

3.2.4.3 Drug distribution of quercetin within nanospheres. Figure 9 shows three nanospheres with quercetin, appearing green entrapped inside the PLGA nanospheres. The polymer shell of these nanospheres appears red as it was labeled with Nile red during the formulation process. The drug, quercetin, can be seen to be uniformly distributed within the nanospheres. This is a critical parameter that would help in uniform drug release from the nanospheres once they are administered in vivo.

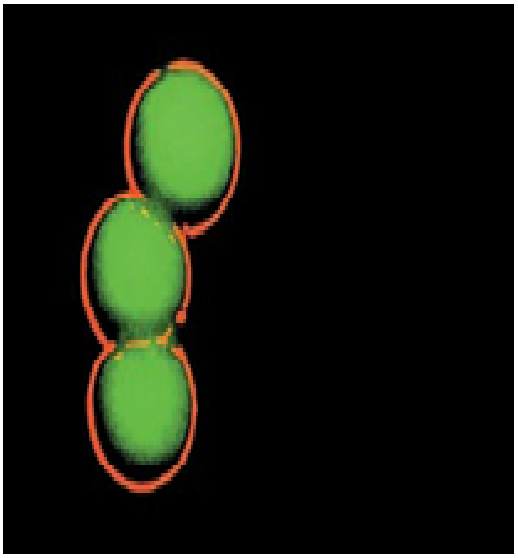

. **Figure 9 . Confocal microscopy scan illustrating the encapsulation and distribution of Quercetin (green fluorescence) within the PLGA nanospheres**.

3.2.4.4 In vitro profile of quercetin release from nanospheres. The release kinetics of quercetin from the PLGA nanospheres was studied for 10 days. Drug release from PLGA nanospheres usually occurs in a biphasic manner, with an initial burst phase followed by a diffusion-controlled slower drug release phase. In our studies, an initial burst phase corresponding to about 10-13% was observed within 1 hour due to the drug desorption and release from the nanosphere surface. A sustained quercetin release to a total of about 65% was found for the nanospheres over the entire period of study, as depicted in the graph shown in Figure 6. The inset in the Figure represents a linear Higuchi plot, which illustrates controlled release of quercetin from the PLGA nanospheres

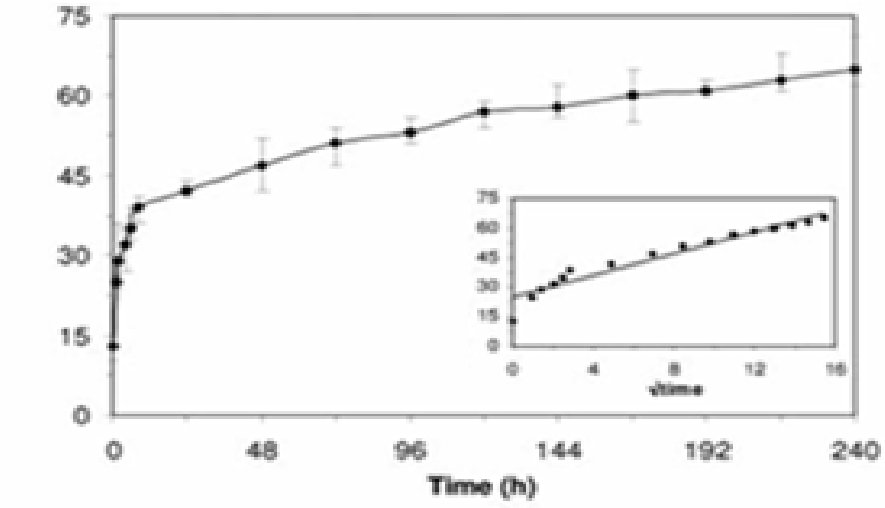

Figure 10 . In vitro profile of release quercetin from PLGA nanospheres in PBS (pH 7.4)

3.3. In-Vitro Anticancer activity

3.3.1 Intracellular uptake studies. Having determined the formulation and characterization of the quercetin-loaded nanospheres, we investigated the ability of these nanospheres to be endocytosed by cells. Figure 11 illustrates an entire panel of the fluorescence microscope images of different cancer cell lines, DU145, PC3 and LNCaP incubated with quercetin-loaded Nile red-labeled PLGA nanospheres for three hours. Our results depict robust uptake of the nanospheres in all three prostate cancer cell lines. Control cells without any quercetin or nanosphere treatment did not show any fluorescence (data not shown). The cells incubated with quercetin-loaded Nile red-labeled nanospheres exhibited either red (due to Nile red) or green (due to quercetin) fluorescence, depending upon the excitation wavelength following rapid internalization and accumulation of quercetin nanospheres by the cancer cells.

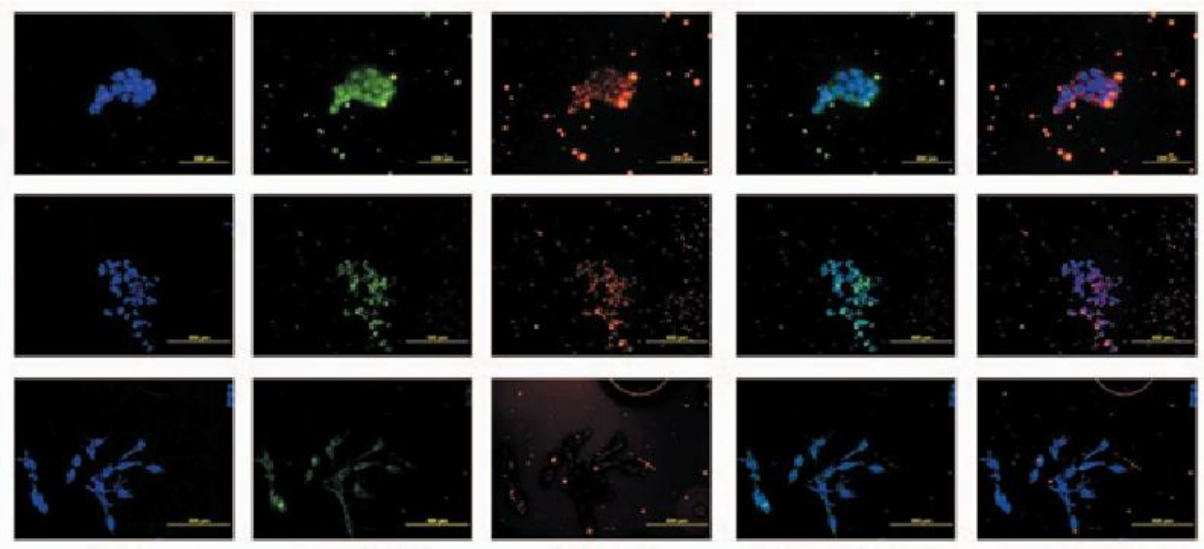

DAPI Quercetin Nile Red DAPI Quercetin merge DAPI Nile red merge

Figure 11. Confocal images of different cell lines incubated with quercetin-loaded nile red-labeled PLGA nanospheres: cell nuclei stained with DAPI, cells showing quercetin in PLGA nanospheres, cells showing nile red-labeled PLGA nanospheres, merged image of DAPI and quercetin in PLGA nanospheres, and merged image of DAPI and nile red-labeled nanospheres

These confocal microscopy images demonstrate the cellular uptake and distribution of quercetin-loaded and Nile red-labeled PLGA nanospheres across three different cancer cell lines: DU 145 (prostate cancer), PC3 (prostate cancer), and LNCaP (prostate cancer).Image Interpretation by Column DAPI (Blue): Highlights the cell nuclei, providing a reference for the location of each cell. Quercetin (Green): **Shows the presence of the drug, Quercetin, which exhibits its own natural green fluorescence in these types** of studies.Nile Red (Red): Marks the PLGA nanosphere carrier itself, which has been labeled with Nile Red dye to track its movement. DAPI-Quercetin Merge: **Confirms that the drug (green) has successfully entered the cell body and is localized around the nuclei (blue).DAPI-Nile Red Merge: Shows the distribution of the nanosphere carriers** (red) relative to the nuclei (blue), demonstrating efficient cellular internalization of the delivery system.

Key Observations The visual evidence suggests that the PLGA nanospheres are effective at delivering Quercetin into the cytoplasm of all three tested cell lines. The overlap in the merged images indicates that the drug is being released or carried directly into the intracellular environment, which is a critical step for its therapeutic anti-cancer potential.

3.3.2 Cell viability assay. Cell viability (MTT) assays were performed using equivalent dosages of free quercetin, quercetin-loaded PLGA nanoparticles and blank PLGA nanoparticles. Untreated cells served as controls. The assay was terminated at 72 hours and colorimetric determination of cell viability was performed. The results of the MTT cell viability assay on prostate cancer cell lines, LNCaP, PC3 and DU145, and a non tumorigenic cell line, PWR1E, are shown in Figure 12. The IC50 of quercetin-loaded PLGA nanoparticles was found to be between 20 µM to 22.5 µM while that of free quercetin ranged from 32 µM to 34 µM among all the cancer cell lines. This accounts for almost 35% reduction in the IC50 value with quercetin-loaded nanoparticles. The assay demonstrated that quercetin-loaded PLGA nanospheres were more effective in arresting cell growth as compared to that shown by free quercetin.

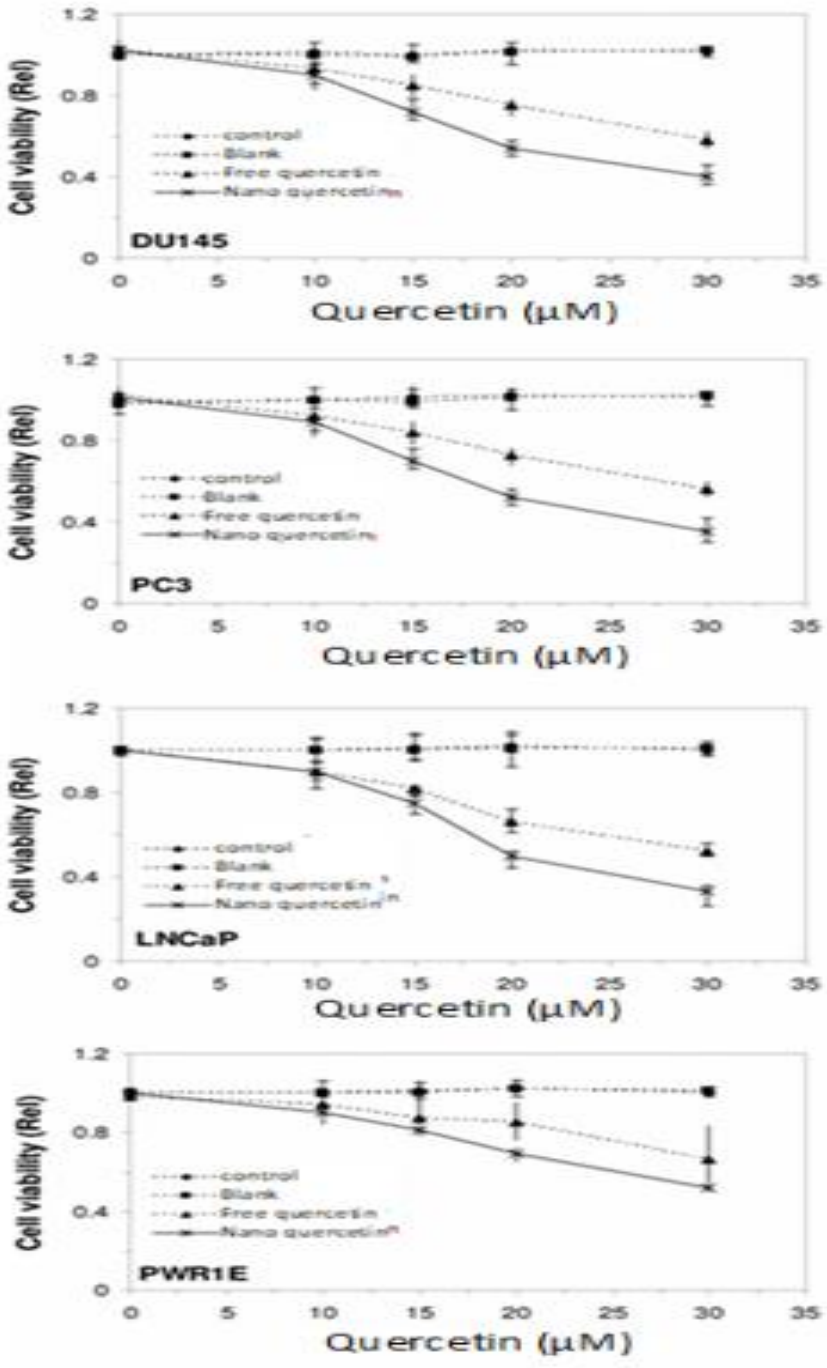

Figure 12 Cell viability (MTT) assay of quercetin-loaded PLGA nanospheres in LNCaP, PC3, DU145 and PWR1E cells. All assays were performed in triplicate, and the mean±standard deviations are shown.

The cell viability assay of PWR1E cells showed that the IC50 of quercetin-loaded PLGA nanoparticles was 31 µM and that of free quercetin was 37 µM. Comparing the IC50 values between non tumorogenic cell line and prostate cancer cell lines, we see a lower IC50 value for the cancer cells than normal cells for both free quercetin and quercetin-loaded PLGA nanoparticles. Furthermore, fewer viable prostate cancer cells were seen for the same concentration of quercetin-loaded nanospheres. This indicates thatquercetin preferentially induces apoptosis in highly proliferating cells, and death is more pronounced in cancer cells than in normal cells.

4. DISCUSSION:

Optimization of the S/O/W Formulation The high encapsulation efficiency (92.14%) and yield (93.04%) suggest that the S/O/W method is superior for Quercetin compared to standard emulsion techniques. By using Ethanol as a non-solvent and 2% PVA as a stabilizer, the polymer precipitated rapidly around the solid drug particles, preventing the drug from leaching into the external aqueous phase. The significant reduction in particle size from ~458 nm to 45 nm as sonication time increased to 2 minutes highlights the importance of high-energy emulsification in overcoming the surface tension required to create nanometer-sized droplets.

2. Molecular State and Compatibility The FTIR results are critical as they prove that the chemical integrity of Quercetin remains intact; no new covalent bonds were formed, indicating a safe physical entrapment. However, the DSC data provides a deeper insight: the disappearance of the Quercetin melting peak at 172°C in the final formulation proves the drug shifted from a crystalline to an amorphous state. This is a major advantage, as amorphous Quercetin has a higher surface area and lower thermodynamic barrier for dissolution, directly addressing the drug's natural challenge of poor aqueous solubility[3]2.

3.Morphology and Internal DistributionThe TEM and Confocal microscopy results complement each other. While TEM confirmed the spherical, smooth nature of the carriers, the green fluorescence of Quercetin within the red-labeled PLGA shells confirms a matrix-type delivery system. This uniform distribution is likely responsible for the controlled release observed, as the drug is not just clumped in the center but spread throughout the polymer chains.4. Release Kinetics and Biological ImplicationsThe biphasic release profile—starting with a 10-13% burst followed by a 65% sustained release over 10 days—is ideal for cancer therapy. The initial burst provides a "loading dose" to the cells, while the sustained phase (following the Higuchi model) ensures a prolonged therapeutic effect. This controlled release, combined with the successful endocytosis observed in DU145, PC3, and LNCaP cells, suggests that the nanospheres bypass cellular efflux pumps that often reject free Quercetin, allowing for higher intracellular accumulation and potential improvement in anti-cancer efficacy[33].

5. CONCLUSION:

The primary objective of this research was to develop and characterize a high-performance delivery system for Quercetin using PLGA nanospheres to overcome its inherent limitations of poor solubility and low bioavailability. The results conclusively demonstrate that the **Solid/Oil/Water (S/O/W) modified emulsion technique** is an exceptionally efficient fabrication route, yielding nanospheres with superior physical and chemical properties.

The study successfully identified that a 2% PVA concentration combined with a precise 2-minute sonication window represents the optimal processing parameters for this system. These conditions produced a remarkably high encapsulation efficiency of 92.14% and a percent yield of 93.04%, figures that significantly exceed traditional emulsion methods. Furthermore, the achievement of a 45 nm mean particle size is a critical milestone; particles in this size range are theoretically ideal for the Enhanced Permeability and Retention (EPR) effect, allowing for passive targeting and accumulation within porous tumor vasculatures.

Characterization through FTIR and DSC provided vital insights into the molecular state of the formulation. The FTIR data confirmed that Quercetin maintains its chemical potency and structure without undergoing deleterious chemical reactions with the PLGA polymer. More importantly, the DSC analysis proved that the encapsulation process successfully converted Quercetin from its native, difficult-to-dissolve crystalline state into an amorphous molecular dispersion. This phase transition is the fundamental reason for the improved aqueous dispersibility of the formulation compared to the free drug.

Therapeutic Potential and Kinetics

The biphasic release profile, which followed the Higuchi model, demonstrates that the nanospheres can provide both an immediate therapeutic dose and a sustained release over a 10-day period. This controlled delivery ensures a prolonged "therapeutic window," which is essential for treating chronic conditions like prostate cancer. The success of the formulation was further validated by Confocal microscopy, which showed a uniform drug distribution, and intracellular uptake studies, which confirmed robust endocytosis across multiple prostate cancer cell lines (DU145, PC3, and LNCaP).

Summary

In conclusion, this Quercetin-loaded PLGA nanosphere system represents a stable, efficient, and biologically active platform for cancer therapy. The S/O/W method effectively "shielded" the drug within a biocompatible polymer, resulting in a formulation that is ready for further in vivo pharmacokinetic and pharmacodynamic evaluation. These findings provide a strong foundation for the potential clinical translation of Quercetin-based nanomedicines in the treatment of solid tumors.

6.REFERENCES:

1. C. C. Akoh and D. B. Min, Food Lipids: Chemistry, Nutrition, and Biotechnology, CRC, 2008.
2. D. B. Min and J. M. Boff, "Lipid oxidation of edible oil," in Food Lipids: Chemistry, Nutrition, and Biotechnology, pp. 335–364, Marcel Dekker, New York, NY, USA, 2002.
3. S. Seki, T. Kitada, T. Yamada, H. Sakaguchi, K. Nakatani, and K. Wakasa, "In situ detection of lipid peroxidation and oxidative DNA damage in non-alcoholic fatty liver diseases," Journal of Hepatology, vol. 37, no. 1, pp. 56–62, 2002.
4. J. W. Baynes and S. R. Thorpe, "Role of oxidative stress in diabetic complications: a new perspective on an old paradigm," Diabetes, vol. 48, no. 1, pp. 1–9, 1999.
5. H. Bartsch and J. Nair, "Oxidative stress and lipid peroxidation-derived DNA-lesions in inflammation driven carcinogenesis," Cancer Detection and Prevention, vol. 28, no. 6, pp. 385–391, 2004.
6. M. D. Gross, "Lipids, oxidation, and cardiovascular disease," in Atherosclerosis and Oxidant Stress, pp. 79–95, Springer, 2008.
7. J. Vercellotti, A. J. S. Angelo, and A. M. Spanier, "Lipid oxidation in foods," in Lipid Oxidation in Food, vol. 500, pp. 1–11, American Chemical Society, 1992.
8. B. Halliwell, S. Chirico, M. A. Crawford, K. S. Bjerve, and K. F. Gey, "Lipid peroxidation: its mechanism, measurement, and significance," American Journal of Clinical Nutrition, vol. 57, no. 5, pp. 715S–724S, 1993.
9. H. Fessi, F. Piusieux, J. P. Devissaguet, N. Ammoury, and S. Benita, "Nanocapsule formation by interfacial polymer depo-sition following solvent displacement," International Journal of Pharmaceutics, vol. 55, no. 1, pp. R1–R4, 1989.
10. L. Mora, K. Y. Chumbimuni-Torres, C. Clawson, L. Her-nandez, L. Zhang, and J. Wang, "Real-time electrochemical monitoring of drug release from therapeutic nanoparticles," Journal of Controlled Release, vol. 140, no. 1, pp. 69–73, 2009.
11. Anjana CHKVLSN. Development and validation of stability indicating RP-UPLC method for the quantification of baloxavir marboxil in the tablet formulation. Int J Pharm Pharm Sci. 2020;12(11):94–99.
12. Babu SRDJV, Sireesha TSM, Anjana Male CHKVLSN, Swathi V, Balaiah S. Evaluation of anticonvulsant activity of ethanolic extract of Gomphrena serrata by using Swiss albino mice. J Pharmacogn Phytochem. 2018;7(4):373–375.
13. Battu G, CKVLSN A, Priya TH, Malleswari VN, Reeshm S. A phytopharmacological review on Vigna species. Pharmanest. 2011;2(1):61–67.
14. Gupta GPKVLSNAMDKPJKSRAAVKPS. Synthesis, properties, and chemical applications of functional nanomaterials: current trends and future perspectives. J Chem Rev. 2025;8(1):1–25.
15. Jyothi N, Reddy BP, Male CH, Swathi S. Comparative assessment of DPPH free radical scavenging activity between Indian medicinal plant extracts of Mansoa alliacea, Kigelia africana, Curcuma aromatica. Degrés. 2025;10(9).
16. Krishna K, Surendra G, Anjana M, Nagini KSK. Phytochemical screening and antimicrobial activity of *Callistemon citrinus* (L.) leaves extracts. Int J Pharm Technol Res. 2012;4(2):700–704.
17. Krishnan NK, Krishnan SG, Male CKVLSN A, et al. Molecular docking and ADMET-based discovery of Glycyrrhiza glabra bioactives as P-glycoprotein inhibitors for combating multidrug resistance. Adv J Chem Sect A. 2025;9(5):773–796.
18. Male CHKA, Nelluri KDD, Bhavana A, Minakshi K, Surendra G, et al. Nutritional aspects and management of Alzheimer's disease and diabetes. Diabetes Alzheimers Dis. 2026;301–369.
19. Male CKA, Varikallu HC, Swapna TS, Dileep N, Prasad S, Nalla S. A case report on scleroderma: a diagnostic dilemma. J Pharm Res Int. 2021;33(40A):251–255.
20. Male NAKSCKVLSN A, Ratala RN, Jyothi GN, et al. A phyto pharmacological comparative review on Curcuma species. Uttar Pradesh J Zool. 2023;44(3):7–15
21. R. C. MacDonald, R. I. MacDonald, B. P. M. Menco, K. Takeshita, N. K. Subbarao, and L. R. Hu, "Small-volume extrusion apparatus for preparation of large, unilamellar vesicles," Biochimica et Biophysica Acta, vol. 1061, no. 2, pp. 297–303, 1991.
22. H. A. Morais, L. M. De Marco, M. C. Oliveira, and M. P. C. Silvestre, "Casein hydrolysates using papain: peptide profile and encapsulation in liposomes," Acta Alimentaria, vol. 34, no. 1, pp. 59–69, 2005.
23. I. B. Afanas'ev, A. I. Dorozhko, A. V. Brodskii, V. A. Kostyuk, and A. I. Potapovitch, "Chelating and free radical scavenging mechanisms of inhibitory action of rutin and quercetin in lipid peroxidation," Biochemical Pharmacology, vol. 38, no. 11,
24. pp. 1763–1769, 1989.
25. M. A. Ebrahimzadeh, S. M. Nabavi, and S. F. Nabavi, "Correlation between the in vitro iron chelating activity and poly phenol and flavonoid contents of some medicinal plants," Pakistan Journal of Biological Sciences, vol. 12, no. 12, pp. 934–938, 2009.

26. F. Ahsan, I. P. Rivas, M. A. Khan, and A. I. Torres Sua´rez, "Targeting to macrophages: role of physicochemical properties of particulate carriers—liposomes and microspheres—on the phagocytosis by macrophages," Journal of Controlled Release, vol. 79, no. 1-3, pp. 29–40, 2002.
27. S. Galindo-Rodriguez, E. Alle´mann, H. Fessi, and E. Doelker, "Physicochemical parameters associated with nanoparticle formation in the salting-out, emulsification-diffusion, and nanoprecipitation methods," Pharmaceutical Research, vol. 21, no. 8, pp. 1428–1439, 2004.
28. X. Song, Y. Zhao, S. Hou et al., "Dual agents loaded PLGA nanoparticles: systematic study of particle size and drug entrapment efficiency," European Journal of Pharmaceutics and Biopharmaceutics, vol. 69, no. 2, pp. 445–453, 2008.
29. X. Song, Y. Zhao, W. Wu et al., "PLGA nanoparticles simultaneously loaded with vincristine sulfate and verapamil hydrochloride: systematic study of particle size and drug entrapment efficiency," International Journal of Pharmaceutics, vol. 350, no. 1-2, pp. 320–329, 2008.
30. O. I. Corrigan and X. Li, "Quantifying drug release from PLGA nanoparticulates," European Journal of Pharmaceutical Sciences, vol. 37, no. 3-4, pp. 477–485, 2009.
31. C. E. Astete and C. M. Sabliov, "Synthesis and characterization of PLGA nanoparticles," Journal of Biomaterials Science, Polymer Edition, vol. 17, no. 3, pp. 247–289, 2006.
32. L. Qi, Z. Xu, X. Jiang, C. Hu, and X. Zou, "Preparation and antibacterial activity of chitosan nanoparticles," Carbohydrate Research, vol. 339, no. 16, pp. 2693–2700, 2004.
33. J. Hu, K. P. Johnston, and R. O. Williams, "Nanoparticle engineering processes for enhancing the dissolution rates of poorly water soluble drugs," Drug Development and Industrial Pharmacy, vol. 30, no. 3, pp. 233–245, 2004.
34. A. Kumari, S. K. Yadav, Y. B. Pakade, B. Singh, and S. C. Yadav, "Development of biodegradable nanoparticles for delivery of quercetin," Colloids and Surfaces B, vol. 80, no. 2, pp. 184–192, 2010.